Structure-preserving discretization of linear port-Hamiltonian systems using mixed FEM approaches *

Cristobal Ponce *,** Yongxin Wu ** Yann Le Gorrec **
Hector Ramirez *

* Departamento de Electrónica, Universidad Técnica Federico Santa María, Valparaíso, Chile. (cristobal.ponces@usm.cl, hector.ramireze@usm.cl).

** FEMTO-ST Institute, École Nationale Supérieure de Mécanique et des Microtechniques, Besançon, France. (cristobal.ponce@femto-st.fr, yongxin.wu@femto-st.fr, yann.le.gorrec@ens2m.fr).

Abstract: This study presents two local approaches for discretizing linear mechanical port-Hamiltonian systems while preserving their structure. These methods employ mixed Finite Element Method (FEM) schemes with weakly enforced Dirichlet and Neumann boundary conditions. The first approach is based on the Hellinger-Reissner variational principle, while the second utilizes the modified Linked Lagrange Multiplier method. Within the framework of each approach, we present two finite-dimensional models, each aligning with distinct representations of the infinite-dimensional system. The results are validated and compared through simulations using a 2D elasticity model as example.

Keywords: Port-Hamiltonian systems; Distributed parameter systems; mixed FEM; Spatial discretization.

1. INTRODUCTION

Port-Hamiltonian systems (PHS) are passive systems that have a structure that can be directly associated with physics (Duindam et al., 2009). Infinite-dimensional PHS were first defined on Stokes-Dirac structures (van der Schaft and Maschke, 2002), but PHS have also been defined in bundle structures and are often called port-Lagrangian systems (PLS) (Ennsbrunner and Schlacher, 2005; Nishida and Yamakita, 2005; Schöberl and Siuka, 2014; Schöberl and Schlacher, 2015). For linear mechanical systems, the main differences with respect to those defined on Stokes-Dirac structures is that the system has an interconnection matrix which is symplectic canonical and the differential dependencies are in the Hamiltonian (for more details see Schöberl and Siuka (2013)). Structurepreserving spatial discretization methods are applied to obtain finite-dimensional PHS that are generally used for simulations and control design purposes. Many discretization techniques have been reported that preserve the interconnection structure and passivity, such as those based on the finite element method (FEM) as the mixed FEM approaches (Golo et al., 2004; Thoma and Kotyczka, 2022; Kinon et al., 2023), partitioned FEM (Cardoso-Ribeiro et al., 2018; Brugnoli et al., 2020, 2022a), exterior calculus FEM (Brugnoli et al., 2022b), and others based on pseudospectral methods (Moulla et al., 2012), finite differences (Trenchant et al., 2018) or finite volumes (Serhani et al., 2018), among others. Regarding mixed FEM, in (Thoma and Kotyczka, 2022) is globally applied the Hellinger-Reissner (H-R) variational principle where Dirichlet and Neumann boundary conditions are weakly imposed. Various other methods for weakly enforcing both Dirichlet and Neumann boundary conditions for linear mechanical systems using FEM include the Lagrange multipliers methods (Babuška, 1973a), penalty method (Babuška, 1973b), Nitsche's method (Embar et al., 2010), Linked Lagrange Multiplier (LLM) method and its modified version (Gerstenberger and Wall, 2010; Baiges et al., 2012), among others. For a more comprehensive review, refer to (Lu et al., 2019). The contributions of this article focuses on the structure-preserving spatial discretization of a class of linear mechanical PHS defined in (Ponce et al., 2023) using two mixed FEM approaches to obtain finite-dimensional port-Hamiltonian and port-Lagrangian models. Similar to (Thoma and Kotyczka, 2022), the first proposed approach is based on the local application of the H-R variational principle, and the second approach relies on the application of the modified LLM method. The document is organized as follows: the considered class of infinite-dimensional PHS is presented in Section 2. Section 3 introduce the discretization approaches and the finitedimensional models for each. Section 4 presents numerical simulations of a 2D elasticity model using the different

^{*} The first author acknowledges financial support from ANID/Becas/Doctorado Nacional/2021-21211290 (Chile) and the ISITE-BFC project - CPHS2D (France). The second author acknowledges the EIPHI Graduate School (contract ANR-17-EURE-0002). The third author acknowledges the MSCA Project MODCONFLEX 101073558 and the ANR Project IMPACTS ANR-21-CE48-0018. The fourth author acknowledges Chilean ANID projects FONDECYT 1231896 and BASAL FB0008.

approaches. Finally, Section 5 provides some conclusions and perspectives for future work.

2. BACKGROUND

The class of infinite-dimensional PHS considered are those presented in (Ponce et al., 2023) associated with a first order differential operator \mathcal{F} .

Definition 1 Let $\mathbf{x} = \{\zeta_1, \dots, \zeta_\ell\}$ be a set of pair-wise perpendicular coordinate axes, $\Omega \subset \mathbb{R}^\ell$ an open set, $v(\mathbf{x}) \in \mathbb{R}^m$ and $w(\mathbf{x}) \in \mathbb{R}^n$ two vector functions. The first order differential operator \mathcal{F} and its formal adjoint \mathcal{F}^* are given by

$$\mathcal{F} w(\mathbf{x}) = P_0 w(\mathbf{x}) + \sum_{k=1}^{\ell} P_k \, \partial_k w(\mathbf{x}) \tag{1}$$

$$\mathcal{F}^* v(\mathbf{x}) = P_0^\top v(\mathbf{x}) - \sum_{k=1}^{\ell} P_k^\top \partial_k v(\mathbf{x})$$
 (2)

with $\partial_k = \partial/\partial \zeta_k$ and $P_0, P_k \in \mathbb{R}^{m \times n}$.

Lemma 1 Consider that Definition 1 holds. Let be $\Omega \subset \mathbb{R}^{\ell}$ an ℓ -dimensional domain, its boundary $\partial \Omega$ and $\bar{\Omega} = \Omega \cup \partial \Omega$ the closure, such that $\mathbf{x} \in \Omega$ and $\mathbf{s} \in \partial \Omega$. Then for any $v(\mathbf{x}) \in \mathbb{R}^m$ and $w(\mathbf{x}) \in \mathbb{R}^n$ defined in $\bar{\Omega}$ we have that

$$\int_{\Omega} v(\mathbf{x})^{\mathsf{T}} \mathcal{F} w(\mathbf{x}) - w(\mathbf{x})^{\mathsf{T}} \mathcal{F}^* v(\mathbf{x}) d\mathbf{x} = \int_{\partial \Omega} w(\mathbf{s})^{\mathsf{T}} \mathcal{P}_{\partial}(\mathbf{s}) v(\mathbf{s}) d\mathbf{s}$$
(3)

with $\mathcal{P}_{\partial}(\mathbf{s}) \in \mathbb{R}^{n \times m}$ a boundary valued matrix given by

$$P_{\partial}(\mathbf{s}) = \sum_{k=1}^{\ell} P_k^{\top} \hat{n}_k(\mathbf{s}) \tag{4}$$

where $\hat{n}_k(\mathbf{s})$ is the component of the outward unit normal vector to the boundary projected on the axis ζ_k .

The considered class of infinite-dimensional linear port-Hamiltonian systems are of the form

$$\underbrace{\begin{bmatrix} \dot{p} \\ \dot{\epsilon} \end{bmatrix}}_{\dot{x}} = \underbrace{\begin{bmatrix} 0 & -\mathcal{F}^* \\ \mathcal{F} & 0 \end{bmatrix}}_{\mathcal{J} = -\mathcal{J}^*} \underbrace{\begin{bmatrix} e_p \\ e_{\epsilon} \end{bmatrix}}_{\delta_x H} + \underbrace{\begin{bmatrix} B_d \\ 0 \end{bmatrix}}_{\mathcal{G}} u_d \tag{5}$$

$$y_d = \mathcal{G}^* \delta_x H = B_d^*(e_p)$$

$$H(p,\epsilon) = \frac{1}{2} \int_{\Omega} p^{\top} \mathcal{M}^{-1} p + \epsilon^{\top} \mathcal{K} \epsilon \, d\mathbf{x}$$
 (6)

and the power exchange with the environment is given by

$$\partial_t H = \int_{\Omega} y_d^{\top} u_d \, d\mathbf{x} + \int_{\partial \Omega} e_p^{\top} \mathcal{P}_{\partial} \, e_{\epsilon} \, d\mathbf{s}$$
 (7)

where $x(\mathbf{x},t) \in \mathbb{R}^{n+m}$ is the state variable, $\mathcal{J} = -\mathcal{J}^*$ is the skew-adjoint differential operator (interconnection operator), B_d is an input map operator, u_d, y_d are the power-conjugated distributed input and output, respectively. The total energy of the system (5) is given by the Hamiltonian $H(p,\epsilon)$, where $\mathcal{M}(\mathbf{x}) = \mathcal{M}(\mathbf{x})^{\top} > 0 \in \mathbb{R}^{n \times n}$ is the distributed mass matrix, and $\mathcal{K}(\mathbf{x}) = \mathcal{K}(\mathbf{x})^{\top} > 0 \in \mathbb{R}^{m \times m}$ is the distributed stiffness matrix. The state variable is composed by $p(\mathbf{x},t) = \mathcal{M}(\mathbf{x})\dot{\mathbf{r}}(\mathbf{x},t) \in \mathbb{R}^n$ which is the generalized momentum with $\mathbf{r}(\mathbf{x},t) \in \mathbb{R}^n$ the generalized displacement field, and $\epsilon(\mathbf{x},t) = \mathcal{F}\mathbf{r}(\mathbf{x},t) \in \mathbb{R}^m$ which is the generalized strain field. The efforts are given by $e_p(\mathbf{x},t) = \delta_p H = \mathcal{M}(\mathbf{x})^{-1} p(\mathbf{x},t) = \dot{\mathbf{r}}(\mathbf{x},t)$ which represents the generalized velocity field, and $e_{\epsilon}(\mathbf{x},t) = \delta_{\epsilon} H = \mathcal{K}(\mathbf{x}) \epsilon(\mathbf{x},t) = \mathcal{K}(\mathbf{x}) \mathcal{F}\mathbf{r}(\mathbf{x},t)$ which represents the generalized stress field.

Definition 2 Consider the infinite-dimensional PHS in (5). Assume that $\partial\Omega = \partial\Omega_D \cup \partial\Omega_N$ and $\partial\Omega_D \cap \partial\Omega_N = \{\phi\}$ with $\{\phi\}$ the empty set, where $\partial\Omega_D$ and $\partial\Omega_N$ are the

portions of the boundary where Dirichlet and Neumann boundary conditions are imposed, respectively. Then, for a mixed boundary problem the second term in (7) can be written equivalently as

$$\int_{\partial\Omega} e_p^{\top} \mathcal{P}_{\partial} \, e_{\epsilon} d\mathbf{s} = \int_{\partial\Omega_N} y_{\tau}^{\top} \tau_{\partial} \, d\mathbf{s} + \int_{\partial\Omega_D} v_{\partial}^{\top} y_v \, d\mathbf{s} \qquad (8)$$

with

$$\tau_{\partial}(\mathbf{s}, t) = \mathcal{P}_{\partial}(\mathbf{s})e_{\epsilon}(\mathbf{s}, t) \quad \text{on } \partial\Omega_{N}$$
 (9)

$$v_{\partial}(\mathbf{s}, t) = e_{p}(\mathbf{s}, t)$$
 on $\partial \Omega_{D}$ (10)

$$y_{\tau}(\mathbf{s},t) = e_{p}(\mathbf{s},t)$$
 on $\partial \Omega_{N}$ (11)

$$y_v(\mathbf{s}, t) = \mathcal{P}_{\partial}(\mathbf{s})e_{\epsilon}(\mathbf{s}, t) \quad \text{on } \partial\Omega_D$$
 (12)

where $\tau_{\partial}(\mathbf{s},t) \in \mathbb{R}^n$ is the imposed generalized boundary traction, $v_{\partial}(\mathbf{s},t) \in \mathbb{R}^n$ is the imposed generalized boundary velocity. Then, the boundary inputs of (5) are given by $u_{\partial}(\mathbf{s},t) = [\tau_{\partial}(\mathbf{s},t)^{\top} \ v_{\partial}(\mathbf{s},t)^{\top}]^{\top}$, and the boundary outputs by $y_{\partial}(\mathbf{s},t) = [y_{\tau}(\mathbf{s},t)^{\top} \ y_{v}(\mathbf{s},t)^{\top}]^{\top}$.

An alternative representation of the system (5)-(6) is presented in (Ponce et al., 2023), where the model has the structure of a field port-Lagrangian system defined as

$$\underbrace{\begin{bmatrix} \dot{p} \\ \dot{\mathbf{r}} \end{bmatrix}}_{\dot{z}} = \underbrace{\begin{bmatrix} 0 & -1 \\ 1 & 0 \end{bmatrix}}_{J=-J^{\top}} \underbrace{\begin{bmatrix} e_{p} \\ e_{r} \end{bmatrix}}_{\delta_{z}H} + \underbrace{\begin{bmatrix} B_{d} \\ 0 \end{bmatrix}}_{\mathcal{G}} u_{d}$$

$$y_{d} = \mathcal{G}^{*} \delta_{z} H = B_{d}^{*}(e_{p})$$
(13)

where $z(\mathbf{x},t) = [p(\mathbf{x},t)^{\top} \ \mathbf{r}(\mathbf{x},t)^{\top}]^{\top} \in \mathbb{R}^{2n}$ is the state variable, the interconnection operator $J = -J^{\top}$ is algebraic (canonical symplectic), and the differential part is now in the Hamiltonian $H(p,\mathbf{r})$ which is given by

$$H(p, \mathbf{r}) = \frac{1}{2} \int_{\Omega} p^{\top} \mathcal{M}^{-1} p + (\mathcal{F} \mathbf{r})^{\top} \mathcal{K} (\mathcal{F} \mathbf{r}) d\mathbf{x}$$
 (14)

where $e_r(\mathbf{x},t) = \mathcal{F}^*(\mathcal{K}(\mathbf{x}) \mathcal{F} \mathbf{r}(\mathbf{x},t))$ is the variational derivative of the Hamiltonian $H(p,\mathbf{r})$ respect to $\mathbf{r}(\mathbf{x},t)$ and represents the generalized internal loads.

3. SPATIAL DISCRETIZATION

This section presents two different two-fields based mixed FEM approaches for discretizing the PHS in (5) with Hamiltonian (6). The first approach is based on the local form of the H-R variational principle, while the second relies on the modified LLM. Since for some applications it may be useful to have the generalized displacements as a state variable, and/or consider it as a boundary input instead of velocities, for each approach we present their adapted versions. The modifications lead us to discretized models with these characteristics and that preserve the structure of the infinite-dimensional PLS in (13).

Remark 1 For any linear mechanical PHS in (5) with \mathcal{F} of dimension $(m \times n)$, a necessary condition to apply the following two-fields based mixed FEM approaches is that $m \geq n$. (Zienkiewicz et al., 2005, Ch.10.4.3).

3.1 Based on H-R variational principle

The discretization approaches in this section are built upon the weak form of (5) originally introduced in (Thoma and Kotyczka, 2022) for the general linear elasticity problem. The local weak form (defined in each finite element e) is given by

$$\delta P_p^e(e_p, e_\epsilon) = \int_{\Omega^e} \delta e_p^e \cdot (\dot{p}^e + \mathcal{F}^* e_\epsilon^e - B_d(u_d^e)) \, d\mathbf{x} \qquad (15)$$
$$+ \int_{\partial \Omega^e_{\epsilon_e}} \delta e_p^e \cdot (\mathcal{P}_{\partial} e_\epsilon^e - \tau_{\partial}^e) \, d\mathbf{s}$$

$$\delta P_{\epsilon}^{e}(e_{p}, e_{\epsilon}) = \int_{\Omega^{e}} \delta e_{\epsilon}^{e} \cdot (\dot{\epsilon}^{e} - \mathcal{F}e_{p}^{e}) d\mathbf{x}$$

$$+ \int_{\partial \Omega_{D}^{e}} \delta e_{\epsilon}^{e} \cdot \mathcal{P}_{\partial}^{\top} (e_{p}^{e} - v_{\partial}^{e}) d\mathbf{s}$$

$$(16)$$

where the superscript $(\cdot)^e$ denotes that the variable is locally defined in the element e.

Proposition 1 The mixed Galerkin discretization of (5) with Neumann and Dirichlet boundary conditions (9) and (10), respectively, based on the weak formulation (15)-(16), using trial and test functions from the same bases

$$e_{p}^{e}(\mathbf{x},t) = N_{p}^{e}(\mathbf{x}) \, \hat{e}_{p}^{e}(t), \, \delta e_{p}^{e}(\mathbf{x},t) = N_{p}^{e}(\mathbf{x}) \, \delta \hat{e}_{p}^{e}(t) \qquad (17)$$

$$e_{\epsilon}^{e}(\mathbf{x},t) = N_{\epsilon}^{e}(\mathbf{x}) \,\hat{e}_{\epsilon}^{e}(t), \,\delta e_{\epsilon}^{e}(\mathbf{x},t) = N_{\epsilon}^{e}(\mathbf{x}) \,\delta \hat{e}_{\epsilon}^{e}(t)$$
 (18)

$$\tau^e_{\partial}(\mathbf{s},t) = N^e_{\tau_{\partial}}(\mathbf{s})\,\hat{\tau}^e_{\partial}(t),\; u^e_d(\mathbf{x},t) = N^e_d(\mathbf{x})\,\hat{u}^e_d(t) \tag{19}$$

$$v_{\partial}^{e}(\mathbf{s},t) = N_{v_{\partial}}^{e}(\mathbf{s}) \, \hat{v}_{\partial}^{e}(t),$$
 (20)

leads to the finite-dimensional PHS of the form

$$\underbrace{\begin{bmatrix} \dot{\hat{p}}(t) \\ \dot{\hat{e}}(t) \end{bmatrix}}_{\dot{\hat{x}}(t)} = \underbrace{\begin{bmatrix} 0 & -\hat{F}^{\top} \\ \hat{F} & 0 \end{bmatrix}}_{J=-J^{\top}} \underbrace{\begin{bmatrix} \hat{e}_{p}(t) \\ \hat{e}_{\epsilon}(t) \end{bmatrix}}_{\nabla_{\hat{x}}\hat{H}(t)} + \underbrace{\begin{bmatrix} \hat{B}_{d} & \hat{B}_{\tau} & 0 \\ 0 & 0 & \hat{B}_{v} \end{bmatrix}}_{\hat{G}} \underbrace{\begin{bmatrix} \hat{u}_{d}(t) \\ \hat{\tau}_{\partial}(t) \\ \hat{v}_{\partial}(t) \end{bmatrix}}_{\hat{u}(t)}$$

$$\hat{y}(t) = \hat{G}^{\top} \nabla_{\hat{x}}\hat{H}(t) = \begin{bmatrix} \hat{B}_{d}^{\top} \hat{e}_{p}(t) \\ \hat{B}_{\tau}^{\top} \hat{e}_{p}(t) \\ \hat{B}_{v}^{\top} \hat{e}_{\epsilon}(t) \end{bmatrix}}_{\hat{y}_{v}(t)} = \begin{bmatrix} \hat{y}_{d}(t) \\ \hat{y}_{\tau}(t) \\ \hat{y}_{v}(t) \end{bmatrix}$$
(21)

where $\hat{p}(t) = \hat{M}_v \hat{e}_p(t)$ and $\hat{\epsilon}(t) = \hat{K}_{\epsilon}^{-1} \hat{e}_{\epsilon}(t)$ are the discrete generalized momentum and strain variables, respectively. The discrete Hamiltonian $\hat{H}(\hat{p}, \hat{\epsilon})$ is given by

$$\hat{H}(\hat{p},\hat{\epsilon}) = \frac{1}{2}\hat{p}(t)^{\top}\hat{M}_v^{-1}\hat{p}(t) + \frac{1}{2}\hat{\epsilon}(t)^{\top}\hat{K}_{\epsilon}\,\hat{\epsilon}(t)$$
(22)

and the energy balance is given by

$$\dot{\hat{H}}(t) = \hat{y}_d(t)^{\top} \hat{u}_d(t) + \hat{y}_{\tau}(t)^{\top} \hat{\tau}_{\partial}(t) + \hat{y}_v(t)^{\top} \hat{v}_{\partial}(t)$$
 (23)
The involved global matrices are obtained by assembling

$$\hat{M}_v = \sum_{\substack{e=1\\Ne}}^{Ne} (L_p^e)^\top \int_{\Omega^e} N_p^e(\mathbf{x})^\top \mathcal{M}(\mathbf{x}) N_p^e(\mathbf{x}) \, d\mathbf{x} \, L_p^e \tag{24}$$

$$\hat{K}_{\epsilon}^{-1} = \sum_{e=1}^{Ne} (L_{\epsilon}^{e})^{\top} \int_{\Omega^{e}} N_{\epsilon}^{e}(\mathbf{x})^{\top} \mathcal{K}(\mathbf{x})^{-1} N_{\epsilon}^{e}(\mathbf{x}) \, d\mathbf{x} \, L_{\epsilon}^{e}$$
 (25)

$$\hat{F}^{\top} = \sum_{e=1}^{Ne} (L_p^e)^{\top} \left(\int_{\Omega^e} (\mathcal{F} N_p^e(\mathbf{x}))^{\top} N_{\epsilon}^e(\mathbf{x}) d\mathbf{x} - \int_{\partial \Omega_D^e} N_p^e(\mathbf{s})^{\top} \mathcal{P}_{\partial}(\mathbf{s}) N_{\epsilon}^e(\mathbf{s}) d\mathbf{s} \right) L_{\epsilon}^e$$
(26)

$$\hat{B}_d = \sum_{\substack{e=1\\N_s}}^{Ne} (L_p^e)^\top \int_{\Omega_e} N_p^e(\mathbf{x})^\top B_d(N_d^e(\mathbf{x})) d\mathbf{x}$$
 (27)

$$\hat{B}_{\tau} = \sum_{e=1}^{Ne} (L_p^e)^{\top} \int_{\partial \Omega_N^e} N_p^e(\mathbf{s})^{\top} N_{\tau_{\partial}}^e(\mathbf{s}) \, d\mathbf{s}$$
 (28)

$$\hat{B}_v = \sum_{e=1}^{Ne} (L_e^e)^\top \int_{\partial \Omega_D^e} N_e^e(\mathbf{s})^\top \mathcal{P}_{\partial}(\mathbf{s})^\top N_{v_{\partial}}^e(\mathbf{s}) \, d\mathbf{s}$$
 (29)

with L_n^e and L_{ϵ}^e the classic global-to-local boolean location matrices of FEM, Ne is the number of elements in the mesh, \hat{M}_v is the discrete mass matrix, \hat{K}_{ϵ} is the discrete strain-based stiffness matrix, \hat{F} is the discretized operator, and \hat{B}_d , \hat{B}_{τ} and \hat{B}_v are the input maps of $\hat{u}_d(t)$, $\hat{\tau}_{\partial}(t)$ and $\hat{v}_{\partial}(t)$, respectively.

Proof. Using Lemma 1 in (15) it becomes

$$\begin{split} \delta P_p^e(e_p,e_\epsilon) &= \int_{\Omega^e} \!\! \delta e_p^e \cdot \dot{p}^e + \delta \dot{\epsilon}^e \cdot e_\epsilon^e - \delta e_p^e \cdot B_d(u_d^e) \, d\mathbf{x} \\ &- \int_{\partial \Omega_D^e} \!\! \delta e_p^e \cdot \mathcal{P}_\partial e_\epsilon^e \, d\mathbf{s} - \int_{\partial \Omega_N^e} \!\! \delta e_p^e \cdot \tau_\partial^e \, d\mathbf{s} \end{split}$$

Then, using $\delta \dot{\epsilon}^e(\mathbf{x},t) = \mathcal{F} \delta e_p^e(\mathbf{x},t) = (\mathcal{F} N_p^e(\mathbf{x})) \delta \hat{e}_p^e(t)$, $\hat{e}_{p}^{e}(t) = L_{p}^{e}\hat{e}_{p}(t)$ with $\hat{e}_{p}(t)$ the global vector that gathers all $\hat{e}_{p}^{e}(t)$ of all elements e (analogously the same to obtain the rest of global vectors $\delta \hat{e}_p(t)$, $\hat{u}_d(t)$, $\hat{\tau}_{\partial}(t)$, the global form of (15) becomes $\delta P_p(e_p, e_\epsilon) = \sum_{e=1}^{Ne} \delta P_p^e(e_p, e_\epsilon) = 0$

$$\delta P_p = \delta \hat{e}_p^{\top} [\hat{M}_v \dot{\hat{e}}_p + \hat{F}^{\top} \hat{e}_{\epsilon} - \hat{B}_d \hat{u}_d - \hat{B}_{\tau} \hat{\tau}_{\partial}] = 0 \qquad (30)$$

Similarly, $\delta P_{\epsilon}(e_p, e_{\epsilon}) = \sum_{e=1}^{Ne} \delta P_{\epsilon}^{e}(e_p, e_{\epsilon}) = 0$ is given by

$$\delta P_{\epsilon} = \delta \hat{e}_{\epsilon}^{\top} [\hat{K}_{\epsilon}^{-1} \dot{\hat{e}}_{\epsilon} - \hat{F} \hat{e}_{p} - \hat{B}_{v} \hat{v}_{\partial}] = 0 \tag{31}$$

where the constitutive relation $\dot{\epsilon}^e(\mathbf{x},t) = \mathcal{K}(\mathbf{x})^{-1}\dot{e}^e_{\epsilon}(\mathbf{x},t)$ was imposed strongly. The Hamiltonian in each element can be expressed as

$$H^e(e_p^e, e_\epsilon^e) = \frac{1}{2} \int_{\Omega^e} (e_p^e)^\top \mathcal{M}(\mathbf{x}) e_p^e + (e_\epsilon^e)^\top \mathcal{K}(\mathbf{x})^{-1} e_\epsilon^e \, d\mathbf{x}$$

then, the total energy of the system is $H=\sum_{e=1}^{Ne}H^e,$ and the discrete Hamiltonian is given by

$$\hat{H}(\hat{e}_p, \hat{e}_\epsilon) = \frac{1}{2} \hat{e}_p^\top \hat{M}_v \hat{e}_p + \frac{1}{2} \hat{e}_\epsilon^\top \hat{K}_\epsilon^{-1} \hat{e}_\epsilon \tag{32}$$

Finally, with the definitions of the discrete generalized momentum and strain variables, equations (30) and (31) define the finite-dimensional PHS in (21), and (32) defines the Hamiltonian in (22).

Corollary 1 Since $e_p(\mathbf{x},t) = \dot{\mathbf{r}}(\mathbf{x},t)$, we define the discrete generalized velocity as $\dot{\hat{r}}(t) = \hat{e}_{p}(t)$. Therefore, the PHS in (21) can be extended to consider it explicitly in the state vector, resulting in

$$\underbrace{\begin{bmatrix} \dot{\hat{p}}(t) \\ \dot{\hat{e}}(t) \\ \dot{\hat{r}}(t) \end{bmatrix}}_{\hat{x}(t)} = \underbrace{\begin{bmatrix} 0 - \hat{F}^{\top} - I \\ \hat{F} & 0 & 0 \\ I & 0 & 0 \end{bmatrix}}_{J=-J^{\top}} \underbrace{\begin{bmatrix} \hat{e}_{p}(t) \\ \hat{e}_{\epsilon}(t) \\ 0 \end{bmatrix}}_{\nabla_{\hat{x}}\hat{H}(t)} + \underbrace{\begin{bmatrix} \hat{B}_{d} \ \hat{B}_{\tau} & 0 \\ 0 & 0 \ \hat{B}_{v} \\ 0 & 0 & 0 \end{bmatrix}}_{\hat{g}} \underbrace{\begin{bmatrix} \hat{u}_{d}(t) \\ \hat{r}_{\partial}(t) \\ \hat{v}_{\partial}(t) \end{bmatrix}}_{\hat{u}(t)}$$

$$\hat{y}(t) = \hat{G}^{\top} \nabla_{\hat{x}} \hat{H}(t) = \begin{bmatrix} \hat{B}_{d}^{\top} \hat{e}_{p}(t) \\ \hat{B}_{\tau}^{\top} \hat{e}_{p}(t) \\ \hat{B}_{\tau}^{\top} \hat{e}_{\epsilon}(t) \end{bmatrix}}_{\hat{g}_{\tau}(t)} = \begin{bmatrix} \hat{y}_{d}(t) \\ \hat{y}_{\tau}(t) \\ \hat{y}_{v}(t) \end{bmatrix}$$
(33)

where I is an identity matrix of appropriate dimensions. The discrete Hamiltonian and the energy balance are the same defined in (22) and (23), respectively.

Now, we present the adapted version of the H-R variational principle to include generalized displacements as states and as boundary inputs $(r_{\partial}(\mathbf{s},t) = \mathbf{r}(\mathbf{s},t) \text{ on } \partial\Omega_D)$. The adapted local weak form of the system (5) is given by

$$\delta W_p^e(\mathbf{r}, e_{\epsilon}) = \int_{\Omega^e} \delta \mathbf{r}^e \cdot (\dot{p}^e + \mathcal{F}^* e_{\epsilon}^e - B_d(u_d^e)) \, d\mathbf{x} \qquad (34)$$
$$+ \int_{\partial \Omega^e_{\epsilon}} \delta \mathbf{r}^e \cdot (\mathcal{P}_{\partial} e_{\epsilon}^e - \tau_{\partial}^e) \, d\mathbf{s}$$

$$\delta W_{\epsilon}^{e}(\mathbf{r}, e_{\epsilon}) = \int_{\Omega^{e}} \delta e_{\epsilon}^{e} \cdot (\epsilon^{e} - \mathcal{F}\mathbf{r}^{e}) d\mathbf{x} + \int_{\partial \Omega_{D}^{e}} \delta e_{\epsilon}^{e} \cdot \mathcal{P}_{\partial}^{\top} (\mathbf{r}^{e} - r_{\partial}^{e}) d\mathbf{s}$$
(35)

The only difference between (15) and (34) is the premultiplied test function. Regarding (16) and (35), the compatibility equation ($\epsilon^e - \mathcal{F}\mathbf{r}^e$) replaces the second dynamic equation of (5) and the boundary contribution is expressed in terms of generalized displacements.

Proposition 2 The mixed Galerkin discretization of (5) with Neumann boundary condition in (9) and Dirichlet boundary condition $r_{\partial}(\mathbf{s},t) = \mathbf{r}(\mathbf{s},t)$ on $\partial\Omega_D$, based on the weak formulation (34)-(35), using trial and test functions (18), (19) and

$$\mathbf{r}^e(\mathbf{x},t) = N_p^e(\mathbf{x})\,\hat{r}^e(t), \ \delta\mathbf{r}^e(\mathbf{x},t) = N_p^e(\mathbf{x})\,\delta\hat{r}^e(t) \qquad (36)$$

$$r_{\partial}^{e}(\mathbf{s},t) = N_{v_{\partial}}^{e}(\mathbf{s})\,\hat{r}_{\partial}^{e}(t),\tag{37}$$

leads to the finite-dimensional PLS of the form

$$\underbrace{\begin{bmatrix} \dot{\hat{p}}(t) \\ \dot{\hat{r}}(t) \end{bmatrix}}_{\dot{\hat{z}}(t)} = \underbrace{\begin{bmatrix} 0 & -I \\ I & 0 \end{bmatrix}}_{J=-J^{\top}} \underbrace{\begin{bmatrix} \hat{e}_{p}(t) \\ \hat{e}_{r}(t) \end{bmatrix}}_{\nabla_{z}\bar{H}(t)} + \underbrace{\begin{bmatrix} \hat{B}_{d} & \hat{B}_{\tau} & \hat{B}_{r} \\ 0 & 0 & 0 \end{bmatrix}}_{\bar{G}} \underbrace{\begin{bmatrix} \hat{u}_{d}(t) \\ \hat{\tau}_{\partial}(t) \end{bmatrix}}_{\bar{u}(t)}$$

$$\bar{y}(t) = \bar{G}^{\top} \nabla_{\bar{z}} \bar{H}(t) = \begin{bmatrix} \hat{B}_{d}^{\top} \hat{e}_{p}(t) \\ \hat{B}_{\tau}^{\top} \hat{e}_{p}(t) \\ \hat{B}^{\top} \hat{e}_{z}(t) \end{bmatrix}}_{\bar{R}^{\top}\hat{e}_{z}(t)} = \begin{bmatrix} \hat{y}_{d}(t) \\ \hat{y}_{\tau}(t) \\ \hat{y}_{r}(t) \end{bmatrix}$$
(38)

with discrete Hamiltonian $\bar{H}(\hat{p},\hat{r})$ given by

$$\bar{H}(\hat{p},\hat{r}) = \frac{1}{2}\hat{p}(t)^{\top}\hat{M}_{v}^{-1}\hat{p}(t) + \frac{1}{2}\hat{r}(t)^{\top}\hat{K}_{r}\hat{r}(t)$$
(39)

and energy balance $\dot{\bar{H}}$ given by

$$\dot{\bar{H}} = \hat{y}_d(t)^\top \hat{u}_d(t) + \hat{y}_\tau(t)^\top \hat{\tau}_{\partial}(t) + \hat{y}_r(t)^\top \hat{r}_{\partial}(t)$$
 (40)

where $\hat{K}_r = \hat{F}^{\top} \hat{K}_{\epsilon} \hat{F}$ is the discrete displacement-based stiffness matrix, $\hat{B}_r = -\hat{F}^{\top} \hat{K}_{\epsilon} \hat{B}_v$ is the input map of $\hat{r}_{\partial}(t)$, I is an identity matrix, and the rest of global matrices are the same previously defined in Proposition 1.

Proof. Analogously to the proof of Proposition 1 we have

$$\delta W_p(\mathbf{r}, e_{\epsilon}) = \delta \hat{r}^{\top} [\hat{M}_v \dot{\hat{e}}_p + \hat{F}^{\top} \hat{e}_{\epsilon} - \hat{B}_d \hat{u}_d - \hat{B}_{\tau} \hat{\tau}_{\partial}] = 0 \quad (41)$$

$$\delta W_{\epsilon}(\mathbf{r}, e_{\epsilon}) = \delta \hat{e}_{\epsilon}^{\top} [\hat{K}_{\epsilon}^{-1} \hat{e}_{\epsilon} - \hat{F} \hat{r} - \hat{B}_{v} \hat{r}_{\partial}] = 0 \tag{42}$$

From (42) we obtain

$$\hat{e}_{\epsilon} = \hat{K}_{\epsilon}(\hat{F}\hat{r} + \hat{B}_{v}\hat{r}_{\partial}) \equiv \hat{K}_{\epsilon}\,\bar{\epsilon} \tag{43}$$

Replacing (43) and $\hat{e}_p(t) = \hat{M}_v^{-1} \hat{p}(t)$ in (32) we obtain

$$\hat{H}(\hat{p},\hat{r}) = \frac{1}{2}\hat{p}^{\mathsf{T}}\hat{M}_{v}^{-1}\hat{p} + \frac{1}{2}\begin{bmatrix}\hat{r}\\\hat{r}_{\partial}\end{bmatrix}^{\mathsf{T}}\begin{bmatrix}\hat{K}_{r} & -\hat{B}_{r}\\-\hat{B}_{r} & \hat{V}_{\partial}\end{bmatrix}\begin{bmatrix}\hat{r}\\\hat{r}_{\partial}\end{bmatrix} \tag{44}$$

where $\hat{V}_{\partial} = \hat{B}_{v}^{\top} \hat{K}_{\epsilon} \hat{B}_{v}$. Then, replacing (43) in (41), and considering that $\dot{\hat{r}}(t) = \hat{e}_{v}(t)$ we obtain the following model

$$\begin{bmatrix} \dot{\hat{p}}(t) \\ \dot{\hat{r}}(t) \end{bmatrix} = \begin{bmatrix} 0 & -I \\ I & 0 \end{bmatrix} \begin{bmatrix} \hat{e}_p(t) \\ \bar{e}_r(t) \end{bmatrix} + \begin{bmatrix} \hat{B}_d & \hat{B}_\tau \\ 0 & 0 \end{bmatrix} \begin{bmatrix} \hat{u}_d(t) \\ \hat{\tau}_{\partial}(t) \end{bmatrix}$$
(45)

where $\hat{e}_p(t) = \hat{M}_v^{-1}\hat{p}(t)$ and $\bar{e}_r(t) = \hat{K}_r\hat{r}(t) - \hat{B}_r\hat{r}_{\partial}(t)$. Finally, with $\bar{H}(\hat{p},\hat{r})$ defined in (39) the model (45) can be equivalently rewritten as (38) with $\hat{e}_r(t) = \hat{K}_r\hat{r}(t)$.

3.2 Based on modified LLM

The modified LLM (Baiges et al., 2012) is a strategy of imposing non-homogeneous Dirichlet boundary conditions

which, similarly to the H-R variational principle, uses the generalized stress field as Lagrange multiplier. To ensure symmetry, an additional term is added to link the generalized stress and displacement fields near to the Dirichlet boundary (in Ω_D) in a least square sense, where $\Omega_D \subset \Omega$ is called the Dirichlet domain and represents the set of all finite elements with at least one node in contact with $\partial\Omega_D$. Considering the above, the local weak form of (5) is given by

$$\delta P_p^e(\dot{\mathbf{r}}, e_{\epsilon}) = \int_{\Omega^e} \delta \dot{\mathbf{r}}^e \cdot (\dot{p}^e + \mathcal{F}^* e_{\epsilon}^e - B_d(u_d^e)) \, d\mathbf{x}$$

$$+ \int_{\partial \Omega_N^e} \delta \dot{\mathbf{r}}^e \cdot (\mathcal{P}_{\partial} e_{\epsilon}^e - \tau_{\partial}^e) \, d\mathbf{s} + \frac{1}{\beta} \int_{\Omega_D^e} \delta \dot{\epsilon}^e \cdot (e_{\epsilon} - \mathcal{K}\epsilon) \, d\mathbf{x}$$

$$(46)$$

$$\delta P_{\epsilon}^{e}(\dot{\mathbf{r}}, e_{\epsilon}) = \frac{1}{\beta} \int_{\Omega_{D}^{e}} \delta e_{\epsilon}^{e} \cdot (\dot{\epsilon}^{e} - \mathcal{F}\dot{\mathbf{r}}^{e}) d\mathbf{x}$$

$$+ \int_{\partial \Omega_{D}^{e}} \delta e_{\epsilon}^{e} \cdot \mathcal{P}_{\partial}^{\top} (\dot{\mathbf{r}}^{e} - v_{\partial}^{e}) d\mathbf{s}$$

$$(47)$$

and the Hamiltonian is written as

$$H^{e}(\dot{\mathbf{r}}, \mathbf{r}, e_{\epsilon}) = H^{e}(\dot{\mathbf{r}}, \mathbf{r}) + \frac{1}{\beta} \left[U^{e}(e_{\epsilon}) - U^{e}(\mathbf{r}) \right]_{\Omega_{D}}$$
(48)

where $U^e(e_{\epsilon})$ and $U^e(\mathbf{r})$ represent the elastic potential energy in Ω_D expressed in terms of e_{ϵ} and \mathbf{r} , respectively.

Remark 2 The modified LLM method has been proved to be stable for any $\beta > 1$ when the interpolation spaces pairs are: (a) equal order interpolation, and (b) the displacement and stress fields being piecewise linear and piecewise constant, respectively (Lu et al., 2019).

Proposition 3 The mixed Galerkin discretization of (5) with Neumann boundary condition in (9) and Dirichlet boundary condition $v_{\partial}(\mathbf{s},t) = \dot{\mathbf{r}}(\mathbf{s},t)$ on $\partial\Omega_D$, based on the weak formulation (46)-(47) and Hamiltonian (48), using trial and test functions (18), (19), (20), (36), leads to the finite-dimensional PHS of the form

$$\underbrace{\begin{bmatrix} \dot{\hat{p}}(t) \\ \dot{\hat{e}}_{\scriptscriptstyle D}(t) \\ \dot{\hat{r}}(t) \end{bmatrix}}_{\dot{\hat{x}}(t)} = \underbrace{\begin{bmatrix} 0 & -\tilde{F}_{\scriptscriptstyle D}^{\top} - I \\ \tilde{F}_{\scriptscriptstyle D} & 0 & 0 \\ I & 0 & 0 \end{bmatrix}}_{J=-J^{\top}} \underbrace{\begin{bmatrix} \hat{e}_{p}(t) \\ \tilde{e}_{\epsilon_{\scriptscriptstyle D}}(t) \\ \tilde{e}_{r}(t) \end{bmatrix}}_{\nabla_{\hat{x}}\tilde{H}(t)} + \underbrace{\begin{bmatrix} \hat{B}_{d} & \hat{B}_{\tau} & 0 \\ 0 & 0 & \tilde{B}_{v} \\ 0 & 0 & 0 \end{bmatrix}}_{\dot{\hat{u}}(t)} \underbrace{\begin{bmatrix} \hat{u}_{d}(t) \\ \hat{\tau}_{\partial}(t) \\ 0 & 0 & 0 \end{bmatrix}}_{\dot{u}(t)}$$

$$(49)$$

$$\tilde{y}(t) = \tilde{G}^{\top}\nabla_{\tilde{x}}\tilde{H}(t) = \begin{bmatrix} \hat{B}_{d}^{\top}\hat{e}_{p}(t) \\ \hat{B}_{\tau}^{\top}\hat{e}_{p}(t) \\ \tilde{B}_{v}^{\top}\hat{e}_{\epsilon_{\scriptscriptstyle D}}(t) \end{bmatrix}}_{\dot{y}_{v}(t)} = \begin{bmatrix} \hat{y}_{d}(t) \\ \hat{y}_{\tau}(t) \\ \tilde{y}_{v}(t) \end{bmatrix}$$

where $\hat{p}(t) = \hat{M}_v \hat{e}_p(t) = \hat{M}_v \dot{\hat{r}}(t)$ is the discrete generalized momentum, and $\tilde{\epsilon}_D(t) = \tilde{K}_{\epsilon_D}^{-1} \tilde{e}_{\epsilon_D}(t)$ is the discrete generalized strain defined only on Ω_D . The discrete Hamiltonian $\tilde{H}(\hat{p}, \tilde{\epsilon}_D, \hat{r})$ is given by

$$\tilde{H}(\hat{p}, \tilde{\epsilon}_{\scriptscriptstyle D}, \hat{r}) = \frac{1}{2} \hat{p}(t)^{\top} \hat{M}_{\scriptscriptstyle V}^{-1} \hat{p}(t) + \frac{1}{2} \tilde{\epsilon}_{\scriptscriptstyle D}(t)^{\top} \tilde{K}_{\epsilon_{\scriptscriptstyle D}} \tilde{\epsilon}_{\scriptscriptstyle D}(t) + \frac{1}{2} \hat{r}(t)^{\top} (\tilde{K}_{\scriptscriptstyle T} - \tilde{K}_{\scriptscriptstyle D}) \hat{r}(t)$$
(50)

and the energy balance is given by

$$\dot{\tilde{H}}(t) = \hat{y}_d(t)^{\top} \hat{u}_d(t) + \hat{y}_{\tau}(t)^{\top} \hat{\tau}_{\partial}(t) + \tilde{y}_v(t)^{\top} \hat{v}_{\partial}(t)$$
 (51)
Some of the involved global matrices are the same defined
in Proposition 1, and the rest are defined as

$$\tilde{K}_{\epsilon_D}^{-1} = \sum_{e=1}^{N_e^D} (L_{\epsilon_D}^e)^{\top} \frac{1}{\beta} \int_{\Omega_D^e} N_{\epsilon}^e(\mathbf{x})^{\top} \mathcal{K}(\mathbf{x})^{-1} N_{\epsilon}^e(\mathbf{x}) \, d\mathbf{x} \, L_{\epsilon_D}^e \quad (52)$$

$$\tilde{K}_{\scriptscriptstyle D} = \sum_{e=1}^{Ne} (L_p^e)^{\top} \frac{1}{\beta} \int_{\Omega_D^e} (\mathcal{F} N_p^e(\mathbf{x}))^{\top} \mathcal{K}(\mathbf{x}) (\mathcal{F} N_p^e(\mathbf{x})) \, d\mathbf{x} \, L_p^e \tag{53}$$

$$\tilde{F}_{\scriptscriptstyle D}^{\top} = \sum_{e=1}^{N_{\scriptscriptstyle D}^e} (L_p^e)^{\top} \frac{1}{\beta} \Biggl(\int_{\Omega_D^e} (\mathcal{F} N_p^e(\mathbf{x}))^{\top} N_{\epsilon}^e(\mathbf{x}) \, d\mathbf{x} - \int_{\partial \Omega_D^e} N_p^e(\mathbf{s})^{\top} \mathcal{P}_{\partial}(\mathbf{s}) N_{\epsilon}^e(\mathbf{s}) \, d\mathbf{s} \Biggr) L_{\epsilon_D}^e$$
(54)

$$\tilde{K}_r = \sum_{e=1}^{Ne} (L_p^e)^{\top} \int_{\Omega_e} (\mathcal{F} N_p^e(\mathbf{x}))^{\top} \mathcal{K}(\mathbf{x}) (\mathcal{F} N_p^e(\mathbf{x})) \, d\mathbf{x} \, L_p^e \quad (55)$$

$$\tilde{B}_{v} = \sum_{e=1}^{N_{e}^{e}} (L_{\epsilon_{D}}^{e})^{\top} \int_{\partial \Omega_{D}^{e}} N_{\epsilon}^{e}(\mathbf{s})^{\top} \mathcal{P}_{\partial}(\mathbf{s})^{\top} N_{v_{\partial}}^{e}(\mathbf{s}) d\mathbf{s}$$
 (56)

with $L_{\epsilon_D}^e$ the global-to-local boolean location matrix that assemble only in the nodes on Ω_D , $N_e^{\scriptscriptstyle D}$ is the number of elements in the mesh on Ω_D , \tilde{K}_{ϵ_D} is the discrete strain-based stiffness matrix on Ω_D , $\tilde{F}_{\scriptscriptstyle D}$ is the discretized operator on Ω_D , $\tilde{K}_{\scriptscriptstyle D}$ is the displacement-based linked stiffness matrix, \tilde{K}_r is the displacement-based stiffness matrix, and \tilde{B}_v is the input map of $\hat{v}_{\partial}(t)$ defined on Ω_D .

Proof. Using Lemma 1 in (46) it becomes

$$\begin{split} \delta P_p^e(\dot{\mathbf{r}},e_\epsilon) &= \int_{\Omega^e} \!\! \delta \dot{\mathbf{r}}^e \cdot \dot{p}^e + \delta \dot{\epsilon}^e \cdot e_\epsilon^e - \delta \dot{\mathbf{r}}^e \cdot B_d(u_d^e) \, d\mathbf{x} \\ - \!\! \int_{\partial \Omega_D^e} \!\! \delta \dot{\mathbf{r}}^e \cdot \mathcal{P}_\partial e_\epsilon^e \, d\mathbf{s} - \!\! \int_{\partial \Omega_N^e} \!\! \delta \dot{\mathbf{r}}^e \cdot \tau_\partial^e \, d\mathbf{s} + \frac{1}{\beta} \!\! \int_{\Omega_D^e} \!\! \delta \dot{\epsilon}^e \cdot (e_\epsilon - \mathcal{K}\epsilon) \, d\mathbf{x} \end{split}$$

Using $\dot{\epsilon}^e(\mathbf{x},t) = \mathcal{F}N_p^e(\mathbf{x})\dot{\hat{r}}^e(t)$, $e_\epsilon^e(\mathbf{x},t) = \mathcal{K}(\mathbf{x})\mathcal{F}N_p^e(\mathbf{x})\hat{r}^e(t)$, and assembling with the location matrices the global form of (46) becomes $\delta P_p(\dot{\mathbf{r}},e_\epsilon) = \sum_{e=1}^{N_e} \delta P_p^e(\dot{\mathbf{r}},e_\epsilon) = 0$ and is given by

$$\delta P_p = \delta \dot{\hat{r}}^{\top} [\hat{M}_v \ddot{\hat{r}} + (\tilde{K}_r - \tilde{K}_{\scriptscriptstyle D}) \hat{r} + \tilde{F}_{\scriptscriptstyle D}^{\top} \tilde{e}_{\epsilon_{\scriptscriptstyle D}} - \hat{B}_d \hat{u}_d - \hat{B}_\tau \hat{\tau}_{\partial}] = 0 \quad (57)$$

Similarly,
$$\delta P_{\epsilon}(\dot{\mathbf{r}}, e_{\epsilon}) = \sum_{e=1}^{N_{e}^{D}} \delta P_{\epsilon}^{e}(\dot{\mathbf{r}}, e_{\epsilon}) = 0$$
 is given by
$$\delta P_{\epsilon} = \delta \tilde{e}_{\epsilon_{D}}^{\top} [\tilde{K}_{\epsilon_{D}}^{-1} \dot{\tilde{e}}_{\epsilon_{D}} - \tilde{F}_{D} \hat{e}_{p} - \tilde{B}_{v} \hat{v}_{\partial}] = 0$$
 (58)

where the constitutive relation $\dot{\epsilon}^e(\mathbf{x},t) = \mathcal{K}(\mathbf{x})^{-1} \dot{e}^e_{\epsilon}(\mathbf{x},t)$ was imposed strongly. The Hamiltonian can be expressed according to (48) as

$$\tilde{H}(\dot{\hat{r}}, \tilde{e}_{\epsilon_D}, \hat{r}) = \frac{1}{2} \dot{\hat{r}}^{\top} \hat{M}_v \dot{\hat{r}} + \frac{1}{2} \tilde{e}_{\epsilon_D}^{\top} \tilde{K}_{\epsilon_D}^{-1} \tilde{e}_{\epsilon_D} + \frac{1}{2} \hat{r}^{\top} (\tilde{K}_r - \tilde{K}_{\scriptscriptstyle D}) \hat{r} \quad (59)$$

Finally, with the definitions of the discrete generalized momentum and strain variables, equations (57) and (58) together with $\dot{\hat{r}}(t) = \hat{e}_p(t)$ define the finite-dimensional PHS in (49), and (59) defines the Hamiltonian in (50).

Now, similarly to (34) and (35), the adapted local weak form based on the modified LLM is given by

$$\delta W_p^e(\mathbf{r}, e_{\epsilon}) = \int_{\Omega^e} \delta \mathbf{r}^e \cdot (\dot{p}^e + \mathcal{F}^* e_{\epsilon}^e - B_d(u_d^e)) \, d\mathbf{x}$$

$$+ \int_{\partial \Omega_N^e} \delta \mathbf{r}^e \cdot (\mathcal{P}_{\partial} e_{\epsilon}^e - \tau_{\partial}^e) \, d\mathbf{s} + \frac{1}{\beta} \int_{\Omega_D^e} \delta \epsilon^e \cdot (e_{\epsilon} - \mathcal{K}\epsilon) \, d\mathbf{x}$$
(60)

$$\delta W_{\epsilon}^{e}(\mathbf{r}, e_{\epsilon}) = \frac{1}{\beta} \int_{\Omega_{D}^{e}} \delta e_{\epsilon}^{e} \cdot (\epsilon^{e} - \mathcal{F}\mathbf{r}^{e}) d\mathbf{x}$$

$$+ \int_{\partial \Omega^{e}} \delta e_{\epsilon}^{e} \cdot \mathcal{P}_{\partial}^{\top} (\mathbf{r}^{e} - r_{\partial}^{e}) d\mathbf{s}$$

$$(61)$$

Proposition 4 The mixed Galerkin discretization of (5) with Neumann boundary condition in (9) and Dirichlet boundary condition $r_{\partial}(\mathbf{s},t) = \mathbf{r}(\mathbf{s},t)$ on $\partial\Omega_D$, based on the weak formulation (60)-(61) and Hamiltonian (48), using trial and test functions from the same bases (18), (19), (36), (37), leads to the finite-dimensional PLS of the form

$$\underbrace{\begin{bmatrix} \dot{\hat{p}}(t) \\ \dot{\hat{r}}(t) \end{bmatrix}}_{\dot{\hat{z}}(t)} = \underbrace{\begin{bmatrix} 0 & -I \\ I & 0 \end{bmatrix}}_{J=-J^{\top}} \underbrace{\begin{bmatrix} \hat{e}_{p}(t) \\ \check{e}_{r}(t) \end{bmatrix}}_{\nabla_{\hat{z}}\check{H}(t)} + \underbrace{\begin{bmatrix} \hat{B}_{d} & \hat{B}_{\tau} & \check{B}_{r} \\ 0 & 0 & 0 \end{bmatrix}}_{\check{G}} \underbrace{\begin{bmatrix} \hat{u}_{d}(t) \\ \hat{\tau}_{\partial}(t) \end{bmatrix}}_{\bar{u}(t)}$$

$$\check{y}(t) = \check{G}^{\top} \nabla_{z}\check{H}(t) = \begin{bmatrix} \hat{B}_{d}^{\top} \hat{e}_{p}(t) \\ \hat{B}_{\tau}^{\top} \hat{e}_{p}(t) \\ \dot{B}_{r}^{\top} \hat{e}_{p}(t) \end{bmatrix}}_{\check{g}_{\tau}(t)} = \begin{bmatrix} \hat{y}_{d}(t) \\ \hat{y}_{\tau}(t) \\ \check{y}_{r}(t) \end{bmatrix}$$
(62)

with discrete Hamiltonian $\check{H}(\hat{p},\hat{r})$ given by

$$\check{H}(\hat{p},\hat{r}) = \frac{1}{2}\hat{p}(t)^{\top}\hat{M}_{v}^{-1}\hat{p}(t) + \frac{1}{2}\hat{r}(t)^{\top}\check{K}_{r}\hat{r}(t)$$
(63)

and energy balance \check{H} given by

$$\dot{H} = \hat{y}_d(t)^\top \hat{u}_d(t) + \hat{y}_\tau(t)^\top \hat{\tau}_{\partial}(t) + \check{y}_r(t)^\top \hat{\tau}_{\partial}(t)$$
 (64)

where $\check{K}_r = (\tilde{K}_r - \tilde{K}_D + \tilde{F}_D^{\top} \tilde{K}_{\epsilon_D} \tilde{F}_D)$ is the discrete displacement based stiffness matrix, $\check{B}_r = -\tilde{F}_D^{\top} \tilde{K}_{\epsilon_D} \tilde{B}_v$ is the input map of $\hat{r}_{\partial}(t)$, I is an identity matrix, and the rest of global matrices are the same previously defined in Proposition 3.

Proof. Analogously following the proof of Proposition 2 but using the weak form (60) and (61).

4. NUMERICAL EXAMPLE

The infinite-dimensional PHS for the 2D general elasticity problem is given by (Ponce et al., 2023, Appendix D.2)

$$\begin{bmatrix}
\dot{p}_{1}(\mathbf{x},t) \\
\dot{p}_{2}(\mathbf{x},t) \\
\dot{\epsilon}_{1}(\mathbf{x},t) \\
\dot{\epsilon}_{2}(\mathbf{x},t) \\
\dot{\epsilon}_{3}(\mathbf{x},t)
\end{bmatrix} = \begin{bmatrix}
0 & 0 & \partial_{1} & 0 & \partial_{2} \\
0 & 0 & 0 & \partial_{2} & \partial_{1} \\
\partial_{1} & 0 & 0 & 0 & 0 \\
0 & \partial_{2} & 0 & 0 & 0 \\
\partial_{2} & \partial_{1} & 0 & 0 & 0
\end{bmatrix} \begin{bmatrix}
e_{p_{1}}(\mathbf{x},t) \\
e_{p_{2}}(\mathbf{x},t) \\
e_{\epsilon_{1}}(\mathbf{x},t) \\
e_{\epsilon_{2}}(\mathbf{x},t) \\
e_{\epsilon_{3}}(\mathbf{x},t)
\end{bmatrix}$$
(65)

with Hamiltonian as (6) whose matrices are given by

$$\mathcal{M} = \begin{bmatrix} \rho h & 0 \\ 0 & \rho h \end{bmatrix} \quad , \quad \mathcal{K} = \frac{Eh}{1 - \nu^2} \begin{bmatrix} 1 & \nu & 0 \\ \nu & 1 & 0 \\ 0 & 0 & \frac{1 - \nu}{2} \end{bmatrix}$$
 (66)

where ρ , E, ν are physical properties of the material and h is the thickness. The displacement field is given by $\mathbf{r}(\mathbf{x},t) = [u_1(\mathbf{x},t) \ u_2(\mathbf{x},t)]^{\top}$ where each component represent the displacement of a point $\mathbf{x} \in \Omega \subset \mathbb{R}^2$ in the direction of the Cartesian coordinate axes ζ_1 and ζ_2 , respectively. For the example we consider a rectangular domain $\Omega = [0, L_h] \times [0, L_v]$ with $L_h = 0.25$ [m], $L_v = 0.02$ [m], h = 0.05 [m], $\rho = 5130$ [kg/m³], E = 29.3 [MPa], $\nu = 0.35$ [-], and the penalty like parameter $\beta = 10$ [-]. The considered second-order triangular mesh is shown in Figure 1, where Ω_D , $\partial\Omega_D$ and $\partial\Omega_N$ are highlighted in blue, green and red, respectively.

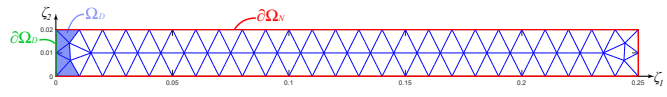


Fig. 1. Dirichlet domain Ω_D , boundary portions $\partial \Omega_D$, $\partial \Omega_N$

To verify that the discretization approaches capture the dynamics of the infinite-dimensional system, the natural frequencies (imaginary part of the eigenvalues) are calculated for each approach and compared with the results delivered by the software Autodesk Inventor, which is considered as reference. For both approaches the interpolation spaces are chosen equal using Lagrange polynomials. Results are shown in Table 1.

	Mode	1	2	3	4	5
Freq. $[Hz]$	Software H-R models LLM models	3.89	23.67	63.52	75.65	117.83

Table 1. Comparison: Software and models.

To validate the effectiveness of the methods to impose boundary conditions on velocity and displacement, the following boundary inputs are applied in $\partial\Omega_D$ for the corresponding models.

$$r_{\partial}(\mathbf{s},t) = \begin{bmatrix} 0\\ 0.01 e^{-50(t-1)^2} \end{bmatrix}, \quad v_{\partial}(\mathbf{s},t) = \dot{r}_{\partial}(\mathbf{s},t) \quad (67)$$

Figure 2 shows the vertical displacement $u_1(\mathbf{x},t)$ of the upper right point of the domain Ω when simulating the finite-dimensional models in Proposition 2 and 4 with boundary input $r_{\partial}(\mathbf{s},t)$, and models in Proposition 1 and 3 with boundary input $v_{\partial}(\mathbf{s},t)$. The same artificial damping was added to all simulations.

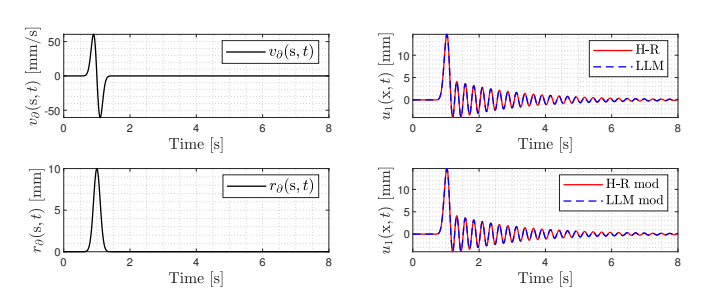


Fig. 2. Comparison: Dirichlet boundary conditions.

From Figure 2 it can be seen that all models exhibit practically the same dynamic response whether applying the Dirichlet boundary input in displacement or velocity. Choosing one model or another will depend on what purposes it is used for. It is worth mentioning that when a first-order triangular mesh is used the results of the H-R based models are more accurate than the LLM based models. It is known that discretization based on displacements are more sensitive to locking. Since the modified LLM approach calculates the elastic potential energy using the generalized displacement field, these discrepancies when using first-order finite elements are likely due to locking issues.

5. CONCLUSION

Two structure-preserving mixed FEM approaches were presented from which four finite-dimensional models were formulated. The approaches are based on the local form of the Hellinger-Reissner variational principle and the Linked Lagrange Multiplier method. Simulations demonstrated nearly identical dynamic responses when displacement or velocity are used as boundary inputs, and also good convergence of the eigenfrequencies compared to the software Autodesk Inventor. Future work includes further investigation regarding of locking in LLM-based models and the extension of these approaches to nonlinear systems.

REFERENCES

Babuška, I. (1973a). The finite element method with Lagrangian multipliers. Numerische Mathematik, 20(3), 179-192. Babuška, I. (1973b). The finite element method with penalty. Mathematics of computation, 27(122), 221–228.

Baiges, J., Codina, R., Henke, F., Shahmiri, S., and Wall, W.A. (2012). A symmetric method for weakly imposing Dirichlet boundary conditions in embedded finite element meshes. International Journal for Numerical Methods in Engineering, 90(5), 636–658.

Brugnoli, A., Cardoso-Ribeiro, F.L., Haine, G., and Kotyczka, (2020).Partitioned finite element method for structured discretization with mixed boundary conditions. PapersOnLine, 53(2), 7557-7562.

Brugnoli, A., Haine, G., and Matignon, D. (2022a). structure-preserving discretization of port-Hamiltonian systems with mixed boundary control. IFAC-PapersOnLine, 55(30), 418-

Brugnoli, A., Rashad, R., and Stramigioli, S. (2022b). Dual field structure-preserving discretization of port-Hamiltonian systems using finite element exterior calculus. Journal of computational physics, 471, 111601.

Cardoso-Ribeiro, F.L., Matignon, D., and Lefevre, L. (2018). structure-preserving partitioned finite element method for the 2D wave equation. IFAC-PapersOnLine, 51(3), 119–124.

Duindam, V., Macchelli, A., Stramigioli, S., and Bruyninckx, H. (2009). Modeling and control of complex physical systems: the port-Hamiltonian approach. Springer Science & Business Media.

Embar, A., Dolbow, J., and Harari, I. (2010). Imposing Dirichlet boundary conditions with Nitsche's method and spline-based finite elements. International journal for numerical methods in engineering, 83(7), 877-898.

Ennsbrunner, H. and Schlacher, K. (2005). On the geometrical representation and interconnection of infinite dimensional port controlled Hamiltonian systems. In Proceedings of the 44th IEEE Conference on Decision and Control, 5263-5268. IEEE

Gerstenberger, A. and Wall, W. (2010). An embedded Dirichlet formulation for 3D continua. International Journal for Numerical

Methods in Engineering, 82(5), 537–563.
Golo, G., Talasila, V., van der Schaft, A., and Maschke, B. (2004). Hamiltonian discretization of boundary control systems. Automatica, 40(5), 757-771.

Kinon, P.L., Thoma, T., Betsch, P., and Kotyczka, P. (2023). Port-Hamiltonian formulation and structure-preserving discretization of hyperelastic strings. arXiv preprint arXiv:2304.10957.

Lu, K., Augarde, C.E., Coombs, W.M., and Hu, Z. (2019). impositions of Dirichlet boundary conditions in solid mechanics: a critique of current approaches and extension to partially prescribed boundaries. Computer Methods in Applied Mechanics and Engineering, 348, 632-659.

Moulla, R., Lefevre, L., and Maschke, B. (2012). Pseudo-spectral methods for the spatial symplectic reduction of open systems of conservation laws. Journal of computational Physics, 231(4), 1272 - 1292.

Nishida, G. and Yamakita, M. (2005). Formal distributed port-Hamiltonian representation of field equations. In *Proceedings of the 44th IEEE Conference on Decision and Control*, 6009–6015.

Ponce, C., Wu, Y., Gorrec, Y.L., and Ramirez, H. (2023). Port-Hamiltonian modeling of multidimensional flexible mechanical structures defined by linear elastic relations. arXiv preprint arXiv:2311.03796.

Schöberl, M. and Schlacher, K. (2015). Lagrangian and port-Hamiltonian formulation for distributed-parameter systems. IFAC-PapersOnLine, 48(1), 610-615.

Schöberl, M. and Siuka, A. (2013). Analysis and comparison of port-Hamiltonian formulations for field theories-demonstrated by means of the Mindlin plate. In $2013\ European\ Control\ Conference$ (ECC), 548-553. IEEE.

Schöberl, M. and Siuka, A. (2014). Jet bundle formulation of infinite-dimensional port-Hamiltonian systems using differential operators. Automatica, 50(2), 607-613.

Serhani, A., Matignon, D., and Haine, G. (2018). preserving finite volume method for 2D linear and non-linear port-Hamiltonian systems. IFAC-PapersOnLine, 51(3), 131-136.

Thoma, T. and Kotyczka, P. (2022). Explicit port-Hamiltonian FEM-models for linear mechanical systems with non-uniform boundary conditions. IFAC-PapersOnLine, 55(20), 499-504.

Trenchant, V., Ramirez, H., Le Gorrec, Y., and Kotyczka, P. (2018). Finite differences on staggered grids preserving the port-Hamiltonian structure with application to an acoustic duct. Journal of Computational Physics, 373, 673–697. van der Schaft, A. and Maschke, B.M. (2002). Hamiltonian formula-

tion of distributed-parameter systems with boundary energy flow. Journal of Geometry and physics, 42(1-2), 166–194. Zienkiewicz, O.C., Taylor, R.L., and Zhu, J.Z. (2005). The finite ele-

ment method: its basis and fundamentals. Sixth edition. Elsevier.